Characterization of the Calcium-activated Chloride Channel in Isolated Guinea-Pig Hepatocytes

SHIN-ICHI KOUMI,* RYOICHI SATO,‡ and TAKUMI ARAMAKI*

From the *First Department of Internal Medicine, Nippon Medical School, Tokyo 113, and ‡the First Department of Internal Medicine, Kinki University School of Medicine, Osaka 589, Japan

ABSTRACT Macroscopic and unitary currents through Ca^{2+}-activated Cl^- channels were examined in enzymatically isolated guinea-pig hepatocytes using whole-cell, excised outside-out and inside-out configurations of the patch-clamp technique. When K^+ conductances were blocked and the intracellular Ca^{2+} concentration ($[Ca^{2+}]_i$) was set at 1 μM (pCa = 6), membrane currents were observed under whole-cell voltage-clamp conditions. The reversal potential of the current shifted by ~60 mV per 10-fold change in the external Cl^- concentration. In addition, the current did not appear when Cl^- was omitted from the internal and external solutions, indicating that the current was Cl^- selective. The current was activated by increasing $[Ca^{2+}]_i$ and was inactivated in Ca^{2+}-free, 5 mM EGTA internal solution (pCa > 9). The current was inhibited by bath application of 9-anthracenecarboxylic acid (9-AC) and 4,4′-diisothiocyanatostilbene-2,2′-disulfonic acid (DIDS) in a voltage-dependent manner. In single channel recordings from outside-out patches, unitary current activity was observed, whose averaged slope conductance was 7.4 ± 0.5 pS (n = 18). The single channel activity responded to extracellular Cl^- changes as expected for a Cl^- channel current. The open time distribution was best described by a single exponential function with mean open lifetime of 97.6 ± 10.4 ms (n = 11), while at least two exponentials were required to fit the closed time distributions with a time constant for the fast component of 21.5 ± 2.8 ms (n = 11) and that for the slow component of 411.9 ± 52.0 ms (n = 11). In excised inside-out patch recordings, channel open probability was sensitive to $[Ca^{2+}]_i$. The relationship between $[Ca^{2+}]_i$ and channel activity was fitted by the Hill equation with a Hill coefficient of 3.4 and the half-maximal activation was 0.48 μM. These results suggest that guinea-pig hepatocytes possess Ca^{2+}-activated Cl^- channels.

Dr. Koumi's present address is the Department of Medicine, Northwestern University Medical School, Chicago, IL, 60611.

Address correspondence to Shin-ichi Koumi, Department of Medicine, Hazaki Saiseikai Hospital, 8968 Hazaki Kashimagun, Ibaragi 314-04, Japan.

J. GEN. PHYSIOL. © The Rockefeller University Press · 0022-1295/94/08/0357/17 $2.00
Volume 104 August 1994 357–373

INTRODUCTION

In a variety of species, the permeability of the hepatocyte plasma membrane to K^+ and Cl^- is known to increase by α_1-adrenergic receptor stimulation with noradrenaline (Haylett and Jenkinson, 1972; Burgess, Claret, and Jenkinson, 1981; DeWitt and Putney, 1984; Field and Jenkinson, 1987). Stimulation of α_1-adrenergic receptors by noradrenaline results in activation of phospholipase C, which hydrolyzes phosphatidyl inositol 4,5-bisphosphate (PIP_2) to inositol 1,4,5-triphosphate (IP_3) and diacylglycerol (DAG) in hepatocytes (Creba, Downes, Hawkins, Brewster, Michell, and Kirk, 1983; Exton, 1988, for review). IP_3 has been shown to stimulate Ca^{2+} mobilization from internal stores by binding a specific receptor on the endoplasmic reticulum, resulting in a release of Ca^{2+} into the cytosol in guinea-pig (Berridge and Irvine, 1984, for review; Burgess, Godfrey, McKinney, Berridge, Irvine, and Putney, 1984; Burgess, Irvine, Berridge, McKinney and Putney, 1984; Taylor and Putney, Jr., 1985) and rat liver (Dawson and Irvine, 1984; Joseph, Thomas, Williams, Irvine, and Williamson, 1984; Joseph and Williamson, 1986). This source of Ca^{2+} can raise free cytosolic Ca^{2+} concentration ($[Ca^{2+}]_i$) (Mauger, Poggioli, Guesdon, and Claret, 1984; Charest, Prpic, Exton, and Blackmore, 1985; Lynch, Blackmore, Charest, and Exton, 1985) and the elevated $[Ca^{2+}]_i$ causes a large increase in the permeability of guinea-pig and rabbit hepatocytes to both K^+ and Cl^- (Field and Jenkinson, 1987). The activation of K^+ and Cl^- conductances by these intermediates was further confirmed in recent studies which showed that internal perfusion of guinea-pig hepatocytes with buffered Ca^{2+} solutions or IP_3 mimicked noradrenaline activation of K^+ and Cl^- conductances (Capiod, Field, Ogden, and Sandford, 1987; Ogden, Capiod, Walker, and Trentham, 1990).

Recently, the patch-clamp technique has been applied to examine membrane K^+ conductances caused by an increase in $[Ca^{2+}]_i$ in isolated hepatocytes. Bear and Petersen (1987) demonstrated Ca^{2+}-activated K^+ channels evoked by L-alanine. The Ca^{2+}-activated K^+ channel in guinea-pig hepatocytes has been evaluated in detail using whole-cell and single channel measurements (Capiod and Ogden, 1989*a*,*b*). In contrast to these detailed studies of Ca^{2+}-activated K^+ channels in guinea-pig hepatocytes, Cl^- conductance evoked by the increase of $[Ca^{2+}]_i$ has not been well examined. The purpose of this study was to characterize the properties of the Ca^{2+}-activated Cl^- current in isolated guinea-pig hepatocytes.

MATERIALS AND METHODS

Cell Preparation

Single guinea-pig hepatocytes were enzymatically dissociated according to the method described previously (Graf, Gautam, and Boyer, 1984; Gautam, Ng, and Boyer, 1987; Koumi, Sato, Nagano, Horikawa, Aramaki, and Okumura, 1991; Koumi, Sato, Horikawa, Aramaki, and Okumura, 1994). Briefly, adult guinea-pigs of either sex weighing 300–400 g were anesthetized with pentobarbitone (60 mg/kg, i.p.), and the portal vein was cannulated. Liver perfusion was initiated with a Ca^{2+}-free solution (first perfusion solution) for 10 min at a flow rate of 5 ml/min. The perfusate was switched to a solution containing 4 mM Ca^{2+} and 0.5 mg/ml of collagenase (type I, Sigma Chemical Co., St. Louis, MO) for 10 min at 10 ml/min (second perfusion solution). The solutions were gassed with 100% O_2 and warmed to 37°C. Following

these perfusions, the liver was excised and then minced in Hank's balanced salt solution (BSS). The cells were filtered through a 150-μm nylon mesh, and washed three times by centrifugation at 100 *g* for 3 min. The cell pellets were resuspended in Hank's BSS. The cells were used within 6 h after the isolation.

Isolated cell viability was assessed by the trypan blue exclusion technique after completion of the isolation procedure. The preparation was discarded if <80% of the cells excluded trypan blue.

Solutions and Chemicals

The first solution perfused via the portal vein cannulation contained (in millimolar): NaCl 140, KCl 5.4, NaH_2PO_4 0.6, Na_2HPO_4 0.4, EGTA (ethylene glycol-bis-(β-aminoethylether) *N,N,N',N'*,-tetraacetate) 0.5, $NaHCO_3$ 4.2, glucose 5, and *N'*-2-hydroxyethylpiperazine-*N'*-2-ethanesulfonic acid (HEPES)-NaOH buffer 9.6, pH 7.2 with NaOH. The second perfusion solution contained (in millimolar): NaCl 140, KCl 5.4, $CaCl_2$ 4.0, NaH_2PO_4 0.6, Na_2HPO_4 0.4, $NaHCO_3$ 4.2, HEPES-NaOH buffer 9.6, and collagenase 0.5 (pH = 7.5). Hank's balanced salt solution (BSS) contained (in millimolar): NaCl 140, KCl 5.4, $CaCl_2$ 1.3, $MgCl_2$ 1.0, $MgSO_4$ 1.7, NaH_2PO_4 0.6, Na_2HPO_4 0.4, $NaHCO_3$ 4.2, glucose 5 (pH = 7.2). The external solution (the standard external) used during whole-cell or excised outside-out patch recordings contained (in millimolar): NaCl 142, $CaCl_2$ 1.8, $MgCl_2$ 2.0, glucose 10, HEPES 8, pH 7.3 with NaOH. Ca^{2+}-free external solution contained (in millimolar): NaCl 142, $MgCl_2$ 2.0, glucose 10, HEPES 8, EGTA 5 (pH = 7.3). Pipette solution (standard internal solution) used during the whole-cell or excised outside-out patch recordings contained (in millimolar): CsOH 150, tetraethylammonium (TEA)-aspartate 42, $MgCl_2$ 1.0, EGTA 5, HEPES 8, TEA-Cl 20, pH 7.3 with TEA-OH. Free Ca^{2+} concentration ($[Ca^{2+}]$) was adjusted to 1 μM by adding $CaCl_2$. In some experiments, *N*-hydroxyethylethylenediaminetriacetic acid (HEDTA) was used as the Ca^{2+} buffer instead of EGTA. The high Cl^- pipette solution used for the excised outside-out patch recording contained (in millimolar): CsCl 128, $MgCl_2$ 1.0, EGTA 5, HEPES 8, TEA-Cl 20 (pH = 7.3 by TEA-OH). Free Ca^{2+} concentration ($[Ca^{2+}]$) was adjusted to 1 μM by adding $CaCl_2$. In excised inside-out patch recordings, the external solution (for the outside-out patch recording) was used for the pipette solution and the internal solution (the high Cl^- pipette solution) was used as the bath solution (cytosolic side). The free Ca^{2+} concentration in each solution was calculated on the basis of apparent stability constants for EGTA to obtain activities ranging from $< 10^{-9}$ M to 1.0×10^{-5} M (Fabiato and Fabiato, 1979).

The recording chamber (0.18 ml) was continuously perfused with bath solution at the perfusion rate of 5 ml/min. Temperature of the bath was monitored and was maintained at 37 ± 1°C using a Peltier thermo-electrical device.

Nifedipine, 9-anthracenecarboxylic acid (9-AC), 4,4'-diisothiocyanatostilbene-2,2'-disulfonic acid (DIDS) and apamin were applied to the external solution in whole-cell experiments. All chemicals were purchased from Sigma Chemical Co.

Electrical Recordings

Membrane currents were recorded using the patch-clamp technique (Hamill, Marty, Neher, Sakmann, and Sigworth, 1981) and an Axopatch-1C amplifier (Axon Instruments, Inc., Foster City, CA). The pipettes were pulled in two stages from hard glass tubing (Narishige Scientific Instruments Laboratories, Tokyo, Japan) using a vertical microelectrode puller (type PE-2, Narishige Scientific Instruments Laboratories) and then fire-polished using a microforge (Model MF-83, Narishige Scientific Instruments Laboratories). Electrodes had resistances of 1.0–1.5 MΩ for whole-cell recording and 6–8 MΩ for single channel recording when filled with appropriate standard internal solutions. Inverted voltage-clamp pulses were applied to the bath

through an Ag-AgCl pellet-KCl agar bridge with the pipette potential maintained at ground level. The head stage of the voltage clamp circuit had an ultra-low bias current operational amplifier. The electrode was connected to the negative input with a feedback resistor of 500 MΩ for recording whole-cell current and 50 GΩ for recording single channel current.

For whole-cell recording, the series resistance arising mainly at the electrode tip was compensated for by summing a fraction of the converted current signal to the command potential and feeding it to the positive input of the operational amplifier. The pipette potential was adjusted to give zero current when the tip of the filled pipette was in the external solution. Series resistance compensation was then done to minimize this capacitative surge. The cell capacitance (C_m) was calculated from the equation:

$$C_m = Q/V \quad (1)$$

where Q is total charge movement determined by integrating the area defined by the capacitative transient in response to +10 mV voltage step. The mean cell capacitance was 28.5 ± 4.2 pF (n = 39) in isolated hepatocytes. The capacitative transient remaining after series resistance compensation was constant throughout the experiment. The leakage current was linear in the range −100 to +50 mV when isolated by using Cl^--free internal and external solutions with internal Cs^+ and TEA. This leakage current has been digitally subtracted from each record. The adequacy of the voltage control had been tested by preliminary experiments monitoring the membrane potential using an independent patch electrode. After gaining access in the whole-cell patch-clamp configuration, myocytes were allowed to "stabilize" electrophysiologically for ~5 min before collecting data.

Single channel currents were monitored with a storage oscilloscope (type 5113, Tektronix, Inc., Beaverton, OR) and were stored continuously on digital audio tape (R-60DM, Maxell, Tokyo, Japan) using a PCM data recording system (RD-100T, TEAC, Tokyo, Japan). The recorded single channel events were reproduced and filtered off-line with a cut-off frequency of 1 KHz through an eight-pole low-pass Bessel filter (48 dB/octave, model 902-LPF, Frequency Devices, Inc., Haverhill, MA), digitized with 14-bit resolution at a sample rate of 10 KHz. The data were analyzed on a computer (PC-9801, NEC, Tokyo, Japan) using locally written analysis programs that are based on the half-amplitude threshold analysis method of Colquhoun and Sigworth (1983). Channel transitions were calculated using an averaging technique for determining channel amplitude. The measurements derived from the channel transitions were collected into histograms to allow an analysis of single channel kinetics. Mean dwell times were determined from the sum of exponential fits to the distributions of open and closed times recorded from patches with only one channel.

Data Analysis

All curve fitting was performed with a non-linear least-square algorithm on a computer (PC-9801, NEC) using custom software. The results are expressed as mean ± SD. Differences between sample means were determined using t test or one-way analysis of variance. A P value < 0.05 was considered statistically significant.

RESULTS

Whole-Cell Cl^- Currents

Fig. 1 *A* shows an example of a whole-cell membrane current family recorded from an isolated guinea-pig hepatocyte after subtraction of linear leakage conductance at 37°C. The original current family was obtained by applying 100-ms duration voltage-clamp steps ranging between −100 mV and +50 mV from a holding

potential of −50 mV. The membrane currents were evoked during voltage-clamp steps. K^+ conductances were blocked by replacement of pipette K^+ with Cs^+ and omitting K^+ from external solution. Nifedipine (5 μM) was added to the external solution. $[Ca^{2+}]_i$ was set at 1 μM (pCa = 6) by using the standard pipette solution. Fig. 1 *B* shows the current-voltage (*I-V*) relationship. The slope conductance measured at 0 mV was 12.6 ± 2.9 nS (n = 17). The reversal potential was ~ −50 mV, which is close to the theoretical Nernst potential for a Cl^- selective channel with external Cl^- concentration ($[Cl^-]_o$) of 150 mM (internal Cl^- concentration $[Cl^-]_i$ = 22 mM). This type of current was observed in 58 out of 67 cells (86.6%). To maintain $[Ca^{2+}]_i$ at abnormally high levels, HEDTA has been shown to be preferable

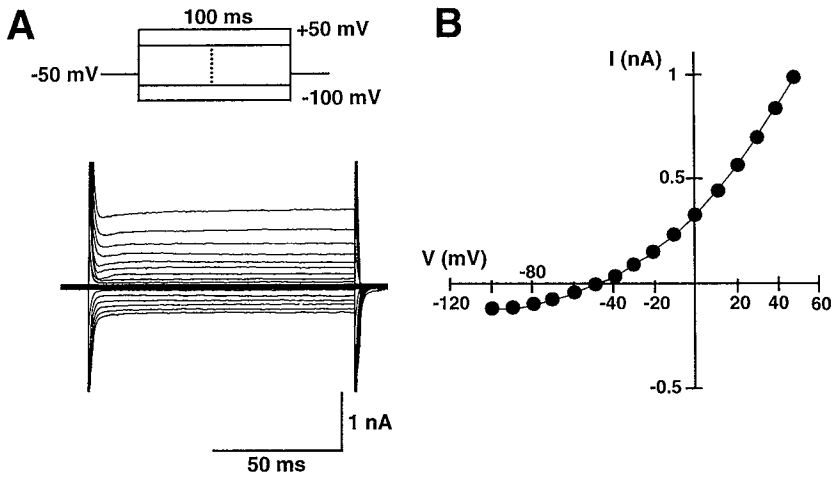

FIGURE 1. Whole-cell membrane currents in isolated guinea-pig hepatocytes. (*A*) Representative family of whole-cell membrane currents recorded in K^+-free solution at 37°C. The pipette solution was the standard internal (pCa = 6, $[Cl^-]$ = 22 mM). The voltage-clamp pulse protocol used to obtain the recordings is depicted in the inset; 100-ms duration pulses to test potentials ranging from −100 to +50 mV in 10-mV increments were applied from a holding potential of −50 mV. Current and time calibration are shown in *A* (*bottom*). (*B*) The current-voltage (*I-V*) relationship derived from the data in *A*. Each point (*circles*) was measured at the end point of the test pulse (100 ms).

to EGTA as a Ca^{2+} buffer (Evans and Marty, 1986). The current relaxation became slow in several cells using the HEDTA-buffered pipette solution (pCa = 6) compared to EGTA, but the averaged time course did not achieve statistical significance (n = 15).

The ionic selectivity of this current was estimated by changing $[Cl^-]_o$ at pCa = 6. $[Cl^-]$ in the pipette solution was 22 mM. Fig. 2 *A* shows the averaged *I-V* relationships in different $[Cl^-]_o$. Decreasing $[Cl^-]_o$ reduced the conductance and shifted the reversal potential to less negative membrane potentials. The averaged reversal potential at $[Cl^-]_o$ = 150 mM was −51.1 ± 3.8 mV (n = 10). The reversal potential was shifted to −30.1 ± 2.6 mV (n = 10) and −0.2 ± 0.3 mV (n = 10) when $[Cl^-]_o$ was decreased to 75 and 22 mM, respectively. The averaged reversal potential was

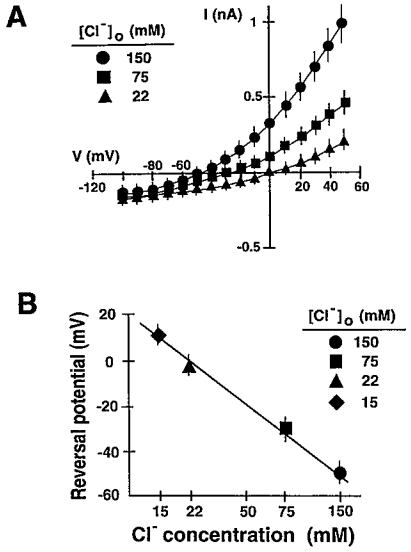

FIGURE 2. Reversal potential measurements for the current. (*A*) The averaged current-voltage (*I-V*) relationships in differ-ent $[Cl^-]$ external solutions. The pipette solution was the standard internal ($[Cl^-]$ = 22 mM, pCa = 6). After obtaining the *I-V* curve in 150 mM $[Cl^-]$ external solution (*circles*), it was switched to 75 mM $[Cl^-]$ (*squares*) and 22 mM $[Cl^-]$ (*triangles*). The vertical bar through each point represents the SD (n = 10 for each). (*B*) The reversal potentials were plotted semilogarithmically as a function of the extracellular Cl^- concentrations ($[Cl^-]_o$). $[Cl^-]_o$ was changed to 150 (*circle*), 75 (*square*), 22 (*triangle*), and 15 mM (*diamond*). The vertical bar through each point represents the SD (n = 10 for each).

plotted against the logarithm of the $[Cl^-]_o$ in Fig. 2 *B*. The best fit to data points (mean ± SD) was obtained with a line having a slope of 60 mV per 10-fold change in $[Cl^-]_o$. In addition, when Cl^- was replaced with aspartate in the internal and external solution, the current did not appear (n = 9, data not shown). These results indicate that this membrane current is highly selective for Cl^- ions.

Ca^{2+}-sensitivity of the Current

The Ca^{2+}-dependence of this Cl^- current was tested using different $[Ca^{2+}]$ pipette solutions. Nifedipine (5 μM) was included in the external solution. The three different Ca^{2+} concentrations were tested; $[Ca^{2+}]_i$ was adjusted to pCa = 6, pCa = 7 or pCa > 9 according to Fabiato and Fabiato (1979). Fig. 3 shows the averaged *I-V* relationships of the three different $[Ca^{2+}]$ pipette solutions. The Cl^- current magnitude became smaller with decreasing $[Ca^{2+}]_i$ without shifting the reversal

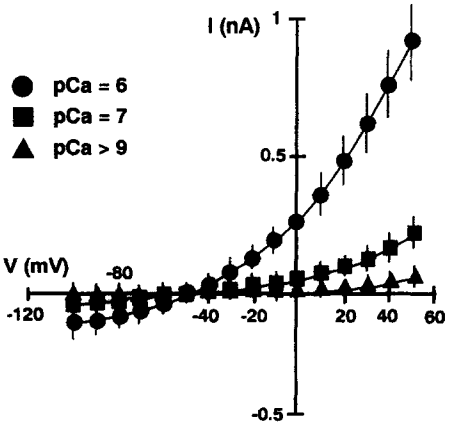

FIGURE 3. Effects of internal Ca^{2+} concentration ($[Ca^{2+}]_i$) on the current. The averaged *I-V* relationships obtained in different $[Ca^{2+}]_i$ are illustrated. pCa was 6 (*circles*), 7 (*squares*), and > 9 (*triangles*). The vertical bar through each point represents the SD (n = 8 for each).

potential. The mean current amplitude was significantly different ($P < 0.01$); the current recorded at pCa = 7 was smaller than that recorded at pCa = 6. The slope conductance became smaller with decreasing $[Ca^{2+}]_i$. The current was inactive at pCa > 9. Similar results were obtained using the Ca^{2+}-free external solution ($n = 5$, not shown).

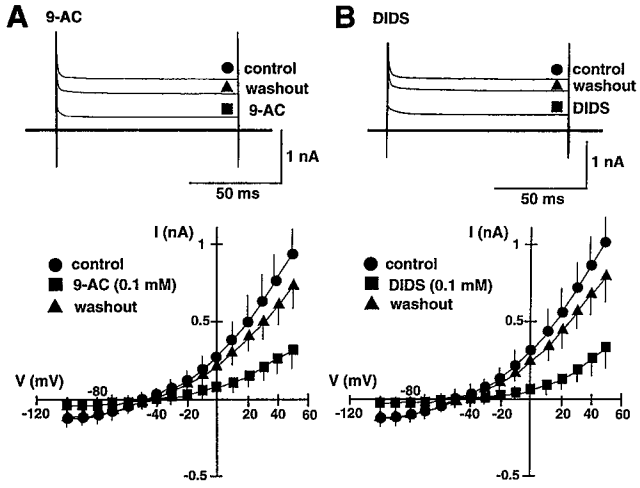

FIGURE 4. Effects of bath application of 9-anthracenecarboxylic acid (9-AC) and 4,4'-diisothiocyanatostilbene-2,2'-disulfonic acid (DIDS) on the current. (*A, top*) Effect of bath application of 9-AC (0.1 mM) on the current. The standard internal solution was used for the pipette solution. Following the measurement of the current in the absence of 9-AC (*circle; control*), 9-AC (0.1 mM) was applied to the external solution. The current was measured during exposure to 9-AC (*square*) and after washout of 9-AC (*triangle*). The current was evoked by test pulses of 100-ms duration to +50 mV from the holding potential of −50 mV. Magnitude of the current was decreased following application of 9-AC. (*A, bottom*) The averaged *I-V* relationships of the current in control (*circles*), during exposure to (*squares*) and after washout of 9-AC (*triangles*). The vertical bar through each point represents the SD ($n = 7$). (*B, top*) Effect of bath application of DIDS (0.1 mM) on the current. After the measurement of the current (*circle; control*), DIDS (0.1 mM) was applied to the external solution. The standard internal solution was used for the pipette solution. 4 min after the application, the current was again measured (*square*). The current was evoked by test pulses of 100-ms duration to +50 mV from the holding potential of −50 mV. Magnitude of the current was inhibited following application of DIDS. (*B, bottom*) The averaged *I-V* relationships of the current in control (*circles*), during exposure to (*squares*) and after washout of DIDS (*triangles*). The vertical bar through each point represents the SD ($n = 7$).

Pharmacological Modification of the Current

9-anthracenecarboxylic acid (9-AC), known to inhibit the Cl^- channel, was applied to the bath solution to test the effect on this current (Fig. 4 *A*). 9-AC (0.1 mM) inhibited the current in seven of seven cells tested. The averaged current amplitude at +50 mV was inhibited to 32.5 ± 7.6% of control ($n = 7$, $P < 0.001$) during exposure to 9-AC

and partially recovered after washout of 9-AC. Inhibition was observed at all voltages tested. The averaged *I-V* relationships before, during exposure to and after washout of 9-AC are shown in the lower panel of Fig. 4 *A*. Effect of DIDS on the Cl^- current was also tested. Fig. 4 *B* shows an example of the effect of externally applied DIDS (0.1 mM) on the Cl^- current. After 3 min exposure to DIDS, the current was drastically reduced (seven of seven cells tested). The current at +50 mV was reduced to 33.8 ± 5.8% (n = 7) of control during application of DIDS. After washout of DIDS, the current magnitude was partially recovered. Fig. 4 *B* (*bottom*) shows the averaged *I-V* relationships.

The voltage-dependence of 9-AC and DIDS block of the current is illustrated in Fig. 5. Fig. 5 *A* shows the fraction of the current remaining after exposure to 9-AC (0.1 mM) at membrane potentials between −20 and +50 mV. The fraction of current remaining in the presence of 9-AC decreased as the membrane potential was made more negative. Similarly, the fraction of current remaining in the presence of DIDS (0.1 mM) reduced with less depolarization (Fig. 5 *B*).

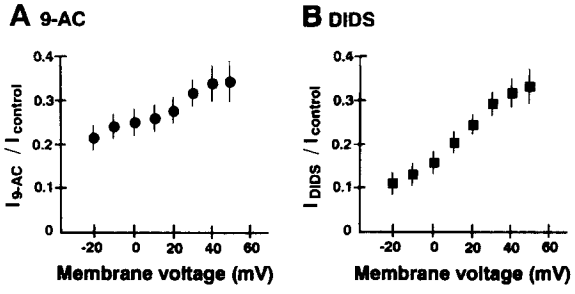

FIGURE 5. Voltage-dependence of current block by 9-anthracenecarboxylic acid (9-AC) and 4,4'-diisothiocyanatostilbene-2,2'-disulfonic acid (DIDS). (*A*) Fraction of the current measured in the presence of 0.1 mM 9-AC ($I_{9\text{-AC}}$) relative to the current measured in the absence of 9-AC ($I_{control}$) plotted as a function of membrane voltage. The standard internal solution was used for the pipette solution. The current was evoked by test pulses of 100-ms duration to various test potentials from the holding potential of −50 mV. The vertical bar through each point represents the SD (n = 6). (*B*) Fraction of the current measured in the presence of 0.1 mM DIDS (I_{DIDS}) relative to the current measured in the absence of DIDS ($I_{control}$) plotted as a function of membrane voltage. The vertical bar through each point represents the SD (n = 6).

In a variety of regions and species, the Ca^{2+}-activated K^+ permeability is inhibited by apamin; a peptide toxin isolated from bee venom (Banks, Brown, Burgess, Burnstock, Claret, Cooks, and Jenkinson, 1979; Burgess et al., 1981; Hugues, Romey, Duval, Vincent, and Lazdunski, 1982; Cook and Haylett, 1985; Blatz and Magleby, 1986*a*). The effect of apamin (50 nM) on the Cl^- current was tested. The current was virtually unchanged by bath application of apamin (data not shown).

Single Cl^- Channel Current in Outside-out Patches

To gain further insight into the channel gating characteristics and modification of the Cl^- current by intracellular Ca^{2+}, we studied the characteristics of single Cl^- channels in the outside-out patch recording. Fig. 6 *A* illustrates examples of individual channel activity recorded at a voltage range between −80 and +80 mV at 37°C. The high Cl^- internal solution was used for the pipette solution ($[Cl^-]_i$ = 150 mM, pCa = 6).

Because this patch contained only one channel, it was used for analysis of single channel gating kinetics. Channel openings occurred in bursts separated by variable interburst intervals at all voltages. We did not detect any time-dependent differences in open probability (P_o) at any potential. The unitary current amplitude was influenced by the membrane voltage. Current traces became flat at ~0 mV, which was the Cl^- equilibrium potential (E_{Cl}). Frequency distributions of the unitary current amplitudes were fit with a Gaussian curve (Fig. 6 *B*). The mean current amplitude for

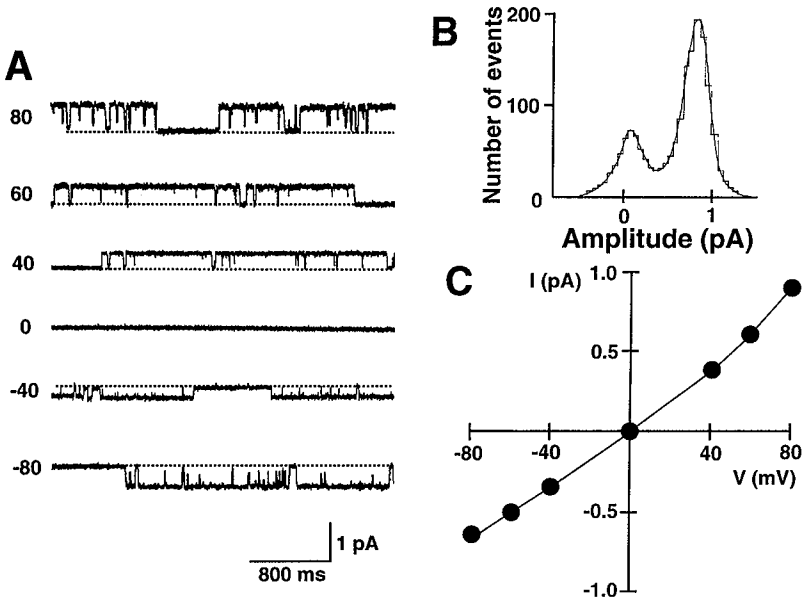

FIGURE 6. The unitary Cl^- current measured by outside-out patch single channel recordings. (*A*) Original recordings of single channel activity of the current. The high Cl^- internal solution was used for the pipette solution ($[Cl^-]_i$ = 150 mM, pCa = 6) in the standard external solution. Channel activity exhibited slow bursting kinetics separated by closed intervals. This patch contained one channel. The holding potential (HP) is indicated to the left of each current trace. The dotted line running in each trace indicates the closed state (baseline level). Currents were low pass filtered at 1 KHz. (*B*) The frequency distribution of the current amplitude at +80 mV. The amplitude of the channel was 0.91 pA at +80 mV. The ordinate gives the number of events and the abscissa is the current amplitude. The distribution is fit with a Gaussian function. (*C*) The *I-V* relationship plotted from the same cell as *A*. Slope conductance is 7.5 pS at 37°C.

the channel was 0.87 ± 0.20 pA (n = 6) at +80 mV. Fig. 6 *C* shows the *I-V* relationship (Fig. 6 *C*). The averaged slope conductance of the channel at 0 mV was 7.4 ± 0.5 pS (n = 18). When single channel activity was measured in different $[Cl^-]_o$ external solutions, the averaged reversal potential of the current shifted by 57 mV per 10-fold change in $[Cl^-]_o$ (not shown), suggesting that the observed single channel current is conducted through Cl^- channels.

Fig. 7 shows the distribution of open and closed times of the channel at +80 mV. Open time distribution was best described by a single exponential function with a mean open lifetime of 97.6 ± 10.4 ms (n = 11). The time constant of the mean open lifetime was plotted as a function of membrane voltage (Fig. 7 *A, bottom*). It did not show significant voltage-dependence. At least two exponentials were required to fit the closed time distributions with a time constant for the fast component of 21.5 ± 2.8 ms (n = 11) and that for the slow component of 411.9 ± 52.0 ms (n = 11). Time constants for the slow component plotted against membrane voltage exhibited weak voltage-dependence; they became greater with more negative membrane potentials. In contrast, time constants for the fast component did not show the voltage-dependence (Fig. 7 *B, bottom*).

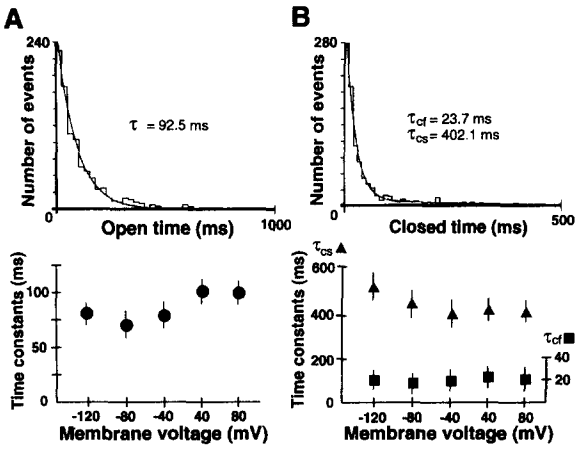

FIGURE 7. Dwell time histograms and the voltage-dependence of the dwell time constants of single Cl^- channel currents in outside-out patch recordings. (*A, top*) Histogram of open times recorded from a representative single channel at +80 mV. The high Cl^- internal solution was used for the pipette solution ($[Cl^-]_i$ = 150 mM, pCa = 6) in the standard external solution. This patch never exhibited more than a single channel during 25 min of continuous recording. Open time distributions were formed from the recording with low-pass filtering at 1 KHz. Open state lifetimes were distributed according to a single exponential function with a time constant (τ_o) of 92.5 ms. (*bottom*) The voltage-dependence of the mean open lifetime. Mean open lifetime (*circles*) was plotted as a function of test voltage. The vertical bar through each point represents the SD (n = 6). (*B, top*) Closed times histogram determined at +80 mV. At least two exponentials were required to fit the closed time distributions with time constants of 23.7 ms for the fast component (τ_{cf}) and 402.1 ms for the slow component (τ_{cs}). (*bottom*) The voltage-dependence of the mean closed times. Mean closed times (τ_{cf}; *squares* and τ_{cs}; *triangles*) were plotted as a function of test voltage. The vertical bar through each point represents the SD (n = 6).

Ca^{2+}- and Voltage-sensitive Nature of the Single Cl^- Channel Current in Inside-out Patches

Modification of the Cl^- channel current by intracellular Ca^{2+} was estimated directly using excised inside-out patch recordings. Single channel activity was measured in different $[Ca^{2+}]$ of bath solution (cytosolic side of the membrane) at a test voltage of +50 mV. Fig. 8 *A* shows examples recorded in different bath solutions. Channel activity was influenced by Ca^{2+} in the bath. Channel open probability (P_o) became greater with increasing $[Ca^{2+}]$ in the bath solution. In contrast, neither mean open

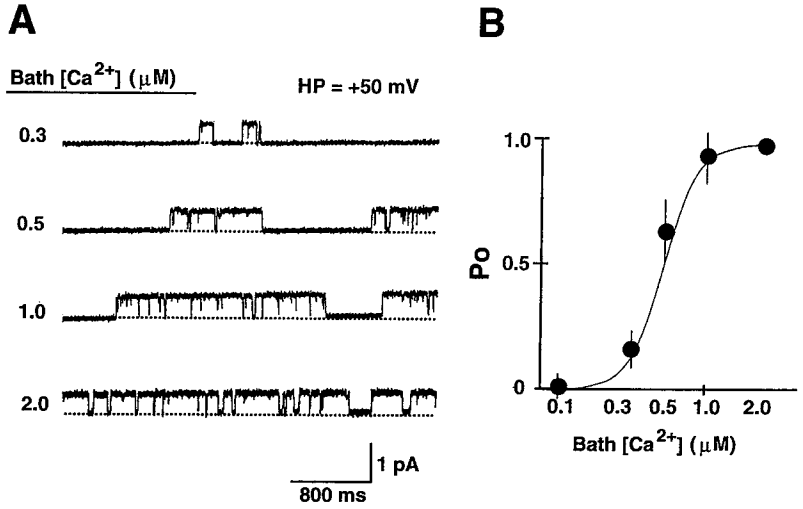

FIGURE 8. Ca^{2+}-dependence of the single channel Cl^- current in inside-out patch recordings. (*A*) Each trace was recorded at the holding potential of +50 mV. Bath solutions (cytosolic side of the membrane) with various concentrations of Ca^{2+} ($[Ca^{2+}]_i$) were applied. $[Ca^{2+}]_i$ is indicated to the left of each current sweep. Data were recorded with low-pass filtering at 1 KHz and digitized at 10 KHz. (*B*) $[Ca^{2+}]_i$-dependent change of channel open probability (P_o) of the outward current. The graph shows the relationship between normalized P_o of the channel and $[Ca^{2+}]_i$ from five different cells. The continuous line is a curve fit to the equation in the text. The Hill coefficient of the fitted curve was 3.4 and the half-maximal inhibition (K_D) was 0.48 μM.

lifetime nor unitary current amplitude was affected. Mean open lifetime was 104.6 ± 12.7 ms (n = 8) recorded at 0.5 μM Ca^{2+} solution and 99.4 ± 11.6 ms (n = 8) at 1 μM Ca^{2+} solution. Channel activity was inhibited extensively in the Ca^{2+}-free solution (pCa > 7). Fig. 8 *B* illustrates the Ca^{2+} concentration-dependence of the channel. P_o at each concentration of Ca^{2+} was estimated. The concentration-dependent activation of the current was fitted by the least-squares method to the Hill equation:

$$\text{Relative } P_o = 1/\{1 + (K_D/[Ca^{2+}])^H\} \quad (2)$$

where K_D is the concentration of Ca^{2+} at the half-maximal channel activation. The relationship between $[Ca^{2+}]$ and the channel activity was fitted by the equation with a Hill coefficient of 3.4 for the channel. The K_D was 0.48 μM.

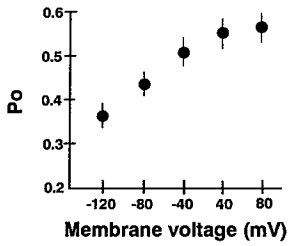

FIGURE 9. Voltage-dependence of open probability of the single channel Cl^- current in inside-out patch recordings. Ca^{2+}-concentration in the bath solution ($[Ca^{2+}]_i$) was set at 0.5 μM. Open probabilities were plotted as a function of membrane voltages between −120 and +80 mV. The vertical bar through each point represents the SD (n = 6).

The voltage-dependence of P_o was evaluated in inside-out patch configurations. Fig. 9 depicts the voltage-dependence of P_o obtained when $[Ca^{2+}]$ in the bath was set at 0.5 μM. Although P_o did not change significantly at positive membrane voltages, it decreased as the membrane potential was made more negative than −40 mV.

DISCUSSION

The major findings in this study are as follows: (*a*) a Cl^- current was found in isolated guinea-pig hepatocytes; (*b*) the Cl^- current was activated by increasing $[Ca^{2+}]_i$; (*c*) The current was inhibited by external application of 9-AC and DIDS in a voltage-dependent manner; (*d*) single channel activity exhibited bursting opening with slow gating kinetics; and (*e*) channel activity in inside-out patch configurations demonstrated a Ca^{2+}-dependent change in open probability. These results indicate that guinea-pig hepatocytes possess Ca^{2+}-activated Cl^- channels.

Relation to Previous Studies

Previous studies showed noradrenaline-induced K^+ and Cl^- permeabilities in guinea-pig hepatocyte plasma membranes (Haylett and Jenkinson, 1972; Burgess et al., 1981). Stimulation of α_1-adrenergic receptors by noradrenaline stimulates phosphatidyl inositol turnover and production of IP_3 which mediates the rise of $[Ca^{2+}]_i$ by release from internal stores (Burgess, Irvine, Berridge, McKinney, and Putney, 1984; Taylor and Putney, Jr., 1985). The elevated $[Ca^{2+}]_i$ activates K^+ and Cl^- conductances in guinea-pig hepatocytes (Field and Jenkinson, 1987; Capiod et al., 1987; Ogden et al., 1990).

The Ca^{2+}-activated K^+ channel has been characterized in detail in guinea-pig hepatocytes (Capiod and Ogden, 1989*a*,*b*). However, the information on the electrophysiological properties of Ca^{2+}-activated Cl^- channel activity is limited. Recently, Capiod and Ogden (1989*a*) predicted that the single Cl^- channels are of very low unitary conductance (< 1 pS) or Cl^- transport is due to a membrane carrier, because the noise increase in spectral analysis associated with the activation of the Cl^- conductance was very small. In contrast, our direct single channel measurements revealed the averaged single channel slope conductance of ~7 pS at 0 mV with symmetrical Cl^- solutions in outside-out patches. This difference may be caused by the following reasons. The single channel conductance appears to be underestimated by the noise analysis; the Ca^{2+}-activated K^+ channel slope conductance has also been predicted to be smaller than the direct single channel measurements (Capiod and Ogden, 1989*a*,*b*). In addition, the single channel recording in the present study was carried out at physiological temperature (37°C), while the noise analysis was performed at 30°C (Capiod and Ogden, 1989*a*). Their analysis at low temperature may also result in the underestimation.

Because the Ca^{2+}-activated Cl^- channel has never been characterized electrophysiologically in hepatocytes, our described channel can be compared with that reported in other systems. The Ca^{2+}-activated Cl^- channel has been reported in secretory epithelial cells (Marty, Tan, and Trautmann, 1984; Evans and Marty, 1986; Evans, Marty, Tan, and Trautmann, 1986; Ishikawa and Cook, 1993), *Xenopus* oocytes (Barish, 1983; Miledi, 1982; Miledi and Parker, 1984), rat exocrine pancreas

(Randriamampita, Chanson, and Trautmann, 1988), salamander photoreceptor membranes (Bader, Bertrand, and Schwartz, 1982), spinal and sensory neurons (Owen, Segal, and Barker, 1984, 1986; Mayer, 1985), skeletal and smooth muscle preparations (Blatz and Magleby, 1986*b*; Byrne and Large, 1987, 1988; Soejima and Kokubun, 1988; Pacaud, Loirand, Lavie, Mironneau, and Mironneau, 1989) and rabbit atrial and ventricular myocytes (Zygmunt and Gibbons, 1991, 1992). There are several similarities between these channels and our described Ca^{2+}-activated Cl^- channel. They are activated by depolarization and the currents are blocked by the anion transport blockers such as DIDS in secretory epithelial cells (Marty et al., 1984; Evans and Marty, 1986; Ishikawa and Cook, 1993), in smooth muscle cells (Pacaud et al., 1989) and rabbit atrial and ventricular cells (Zygmunt and Gibbons, 1991, 1992). However, our described Ca^{2+}-activated Cl^- channel differs from these channels in its sensitivity to Ca^{2+}. The Cl^- conductance in rat lacrimal cells becomes active when $[Ca^{2+}]_i$ exceeds 0.5 μM (Evans and Marty, 1986) and pancreatic acinar cells Cl^- conductances require $[Ca^{2+}]_i > 1$ μM to activate (Randriamampita et al., 1988), levels higher than our described Ca^{2+}-activated Cl^- channel. In contrast, the Cl^- channel in sheep parotid secretory cells is sensitive to $[Ca^{2+}]_i < 0.01$ μM (Ishikawa and Cook, 1993).

Conductance and Gating Properties of the Channel

In physiological solutions, the mean whole-cell current amplitude at 0 mV (which is 50 mV positive to the Cl^- reversal potential) was ~0.25 nA. Because the mean calculated cell capacitance was 28.5 pF, the current amplitude can be estimated as 8.8 pA/pF. With a cell surface area of ~ 1,256 μm^2 (corresponding to the radius of 10 μm for a spherical cell), the current amplitude can be estimated to be 0.20 $pA/\mu m^2$ from the whole-cell measurement. In single channel experiments, the patch membrane area can be estimated using a patch membrane area and the pipette resistance (Sakmann and Neher, 1983). Because 6–8 MΩ resistance pipettes were used, the patch membrane area can be calculated as ~2 μm^2. At a test potential 50 mV positive to the reversal potential, the mean unitary current amplitude was 0.5 pA. Using these values, the calculated mean single channel current was 0.25 $pA/\mu m^2$. The value is close to that obtained from whole-cell estimation.

Our described Ca^{2+}-activated Cl^- channel exhibited slow bursting kinetics separated by interburst periods. The channel may have the one open-channel state, because amplitude histograms of single channel currents contained a single open peak and open time distributions were best described by a single exponential function. In contrast, the channel may have at least two closed states because of the double exponential fitting of the closed time distributions. Although the mean open lifetimes did not show significant voltage-dependence, the mean closed times for the slow component became greater with hyperpolarizing membrane potentials. This may contribute to the voltage-dependent decrease of channel P_o. When $[Ca^{2+}]_i$ was set at 0.5 μM, the voltage-dependent decrease of P_o was observed. This finding suggests that the channel is modulated by both intracellular Ca^{2+} and the membrane voltage.

Physiological Implications

Although ionic basis of the resting membrane potential of the hepatocyte has not been well established, it has been shown that the plasma membrane of the hepatocyte has a relatively high Na^+ and Cl^- permeability compared to that of excitable cells (Claret and Mazet, 1972; Graf, Henderson, Krumpholz, and Boyer, 1987). Capiod and Ogden (1989*a*) demonstrated that Cl^- ions contribute ~80% of resting membrane conductance. Thus, change in Cl^- permeability can affect the transmembrane potential. On the other hand, the resting level of $[Ca^{2+}]_i$ is 0.1–0.2 μM in hepatocytes (Orrenius, Nicotera, and Bellomo, 1987; Ogden et al., 1990). At this level of $[Ca^{2+}]_i$, the Ca^{2+}-activated Cl^- channel is almost inactive. An elevation of $[Ca^{2+}]_i$ beyond this level by α_1-adrenergic stimulation with noradrenaline causes the activation of Cl^- channel. The previously reported Ca^{2+}-activated K^+ channel also becomes active at $[Ca^{2+}]_i$ higher than 0.3 μM (Capiod and Ogden, 1989*b*). However, previous studies showed that the noradrenaline-induced increase of conductance to Cl^- is a five- to eightfold larger than K^+ conductance (Capiod and Ogden, 1987, 1989*a*), suggesting that the Ca^{2+}-activated Cl^- channel may play a major role in determining transmembrane potential. In hepatocytes, membrane potential is important in regulating metabolic function and membrane transport processes such as gluconeogenesis (Friedmann and Dambach, 1980), Na^+-alanine and bile salts uptake (Edmondson, Miller, and Lumeng, 1985; Kristensen, 1986) and amino acid and taurocholate transport (Wondergem and Harder, 1980; Meier, Meier-Abt, Barrett, and Boyer, 1984). In addition to mediating these processes, the Ca^{2+}-activated Cl^- channel may play a role in preventing membrane depolarization. However, the major role of the channel is yet unknown. Further electrophysiological studies related to the metabolic and transport functions are likely to provide important insights into the physiological role of the channel.

The authors wish to thank Dr. Ruth L. Martin (University of Chicago) and Dr. Robert G. Tsushima (Northwestern University Medical School) for their valuable comments on the manuscript and to thank Professor Hidemasa Okumura (Nippon Medical School) for encouraging the authors to attempt these studies of isolated hepatocytes.

Original version received 1 November 1993 and accepted version received 16 March 1994.

REFERENCES

Bader, C. R., D. Bertrand, and E. A. Schwartz. 1982. Voltage-activated and calcium-activated currents studied in solitary rod inner segments from the salamander retina. *Journal of Physiology.* 331:253–284.

Banks, B. E. C., C. Brown, G. M. Burgess, G. Burnstock, M. Claret, T. M. Cooks, and D. H. Jenkinson. 1979. Apamin blocks certain neurotransmitter induced increases in potassium permeability. *Nature.* 282:415–417.

Barish, M. E. 1983. A transient calcium-dependent chloride current in the immature *Xenopus* oocytes. *Journal of Physiology.* 342:309–325.

Bear, C. E., and O. H. Petersen. 1987. L-alanine evokes opening of single Ca^{2+}-activated K^+ channels in rat liver cells. *Pflügers Archiv.* 410:342–344.

Berridge, M. J., and R. F. Irvine. 1984. Inositol triphosphate, a novel second messenger in cellular signal transduction. *Nature.* 312:315–321.

Blatz, A. L., and K. L. Magleby. 1986*a*. Single apamin-blocked Ca-activated K^+ channels of small conductance in cultured rat skeletal muscle. *Nature.* 323:718–720.

Blatz, A. L., and K. L. Magleby. 1986*b*. Quantitative description of three modes of activity of fast chloride channels from rat skeletal muscle. *Journal of Physiology.* 378:141–174.

Burgess, G. M., M. Claret, and D. H. Jenkinson. 1981. Effects of quinidine and apamin on the calcium-dependent potassium permeability of mammalian hepatocytes and red cells. *Journal of Physiology.* 317:67–90.

Burgess, G. M., P. P. Godfrey, J. S. McKinney, M. J. Berridge, R. F. Irvine, and J. W. Putney, Jr. 1984. The second messenger linking receptor activation to initial Ca^{2+} release in liver. *Nature.* 309:63–66.

Burgess, G. M., R. F. Irvine, M. J. Berridge, J. S. McKinney, and J. W. Putney, Jr. 1984. Actions of inositol phosphates on Ca^{2+} pools in guinea-pig hepatocytes. *Biochemical Journal.* 224:741–746.

Byrne, N. G., and W. A. Large. 1987. Action of noradrenaline on single smooth muscle cells freshly dispersed from the rat anococcygeus muscle. *Journal of Physiology.* 389:513–525.

Byrne, N. G., and W. A. Large. 1988. Membrane ionic mechanisms activated by noradrenaline in cells isolated from the rabbit portal vein. *Journal of Physiology.* 404:557–573.

Capiod, T., A. C. Field, D. C. Ogden, and C. A. Sandford. 1987. Internal perfusion of guinea-pig hepatocytes with buffered Ca^{2+} or inositol 1,4,5-triphosphate mimics noradrenaline activation of K^+ and Cl^- conductances. *FEBS Letters.* 217:245–252.

Capiod, T., and D. C. Ogden. 1989*a*. Properties of membrane ion conductances evoked by hormonal stimulation of guinea-pig and rabbit isolated hepatocytes. *Proceedings of the Royal Society of London B Biological Sciences.* 236:187–201.

Capiod, T., and D. C. Ogden. 1989*b*. The properties of calcium-activated potassium ion channels in guinea-pig isolated hepatocytes. *Journal of Physiology.* 409:285–295.

Charest, R., V. Prpic, J. H. Exton, and P. F. Blackmore. 1985. Stimulation of inositol triphosphate formation in hepatocytes by vasopressin, adrenaline and angiotensin II and its relationship to changes in cytosolic free Ca^{2+}. *Biochemical Journal.* 227:79–90.

Claret, M., and J. L. Mazet. 1972. Ionic fluxes and permeabilities of cell membranes in rat liver. *Journal of Physiology.* 223:279–295.

Colquhoun, D., and F. J. Sigworth. 1983. Fitting and statistical analysis of single-channel records. *In* Single-Channel Recording. B. Sakmann, and E. Neher, editors. Plenum Publishing Corp., New York, NY. 191–263.

Cook, N. S., and D. G. Haylett. 1985. Effect of apamin, quinine and neuromuscular blockers on Ca^{2+}-activated K^+ channels in guinea-pig hepatocytes. *Journal of Physiology.* 358:373–394.

Creba, J. A., C. P. Downes, P. T. Hawkins, G. Brewster, R. H. Michell, and C. J. Kirk. 1983. Rapid breakdown of phosphatidylinositol 4-phosphate and phosphatidyl-inositol 4,5-bisphosphate in rat hepatocytes stimulated by vasopressin and other Ca^{2+}-mobilizing hormones. *Biochemical Journal.* 212:733–747.

Dawson, A. P., and R. F. Irvine. 1984. Inositol(1,4,5)triphosphate-promoted Ca^{2+} release from microsomal fractions of rat liver. *Biochemical and Biophysical Research Communications.* 120:858–864.

DeWitt, L. M., and J. M. Putney. 1984. α-adrenergic stimulation of K^+ efflux in guinea-pig hepatocytes may involve Ca^{2+} influx and Ca^{2+} release. *Journal of Physiology.* 346:395–407.

Edmondson, J. W., B. A. Miller, and L. Lumeng. 1985. Effect of glucagon on hepatic taurocholate uptake: relationship to membrane potential. *American Journal of Physiology.* 249:G427–G433.

Evans, M. G., and A. Marty. 1986. Calcium-dependent chloride currents in isolated cells from rat lacrimal glands. *Journal of Physiology.* 378:437–460.

Evans, M. G., A. Marty, Y. P. Tan, and A. Trautmann. 1986. Blockage of Ca-activated Cl conductance by furosemide in rat lacrimal glands. *Pflügers Archiv.* 406:65–68.

Exton, J. H. 1988. Role of phosphoinositides in the regulation of liver function. *Hepatology.* 8:152–166.

Fabiato, A., and F. Fabiato. 1979. Calculator programs for computing the composition of the solutions containing multiple metals and ligands used for experiments in skinned muscle cells. *Journal de Physiologie* 75:463–505.

Field, A. C., and D. H. Jenkinson. 1987. The effect of noradrenaline on the ion permeability of isolated mammalian hepatocytes, studied by intracellular recording. *Journal of Physiology.* 392:493–512.

Friedmann, N., and G. Dambach. 1980. Antagonistic effect of insulin on glucagon-evoked hyperpolarization. A correlation between changes in membrane potential and gluconeogenesis. *Biochimica et Biophysica Acta.* 596:180–185.

Gautam, A., O. C. Ng, and J. L. Boyer. 1987. Isolated rat hepatocyte couplets in short-term culture: structural characteristics and plasma membrane reorganization. *Hepatology.* 7:216–223.

Graf, J., J. A. Gautam, and J. L. Boyer. 1984. Isolated rat hepatocyte couplets: a primary secretory unit for electrophysiologic studies of bile secretory function. *Proceedings of the National Academy of Sciences, USA.* 81:6516–6520.

Graf, J., R. M. Henderson, B. Krumpholz, and J. L. Boyer. 1987. Cell membrane and transepithelial voltages and resistances in isolated rat hepatocyte couplets. *Journal of Membrane Biology.* 95:241–254.

Hamill, O. P., A. Marty, E. Neher, B. Sakmann, and F. J. Sigworth. 1981. Improved patch-clamp technique for high resolution current recording from cell and cell-free membrane patches. *Pflügers Archiv.* 391:85–100.

Haylett, D. G., and D. H. Jenkinson. 1972. Effects of noradrenaline on potassium efflux, membrane potential and electrolyte levels in tissue slices prepared from guinea-pig liver. *Journal of Physiology.* 225:721–750.

Hugues, M., G. Romey, D. Duval, J.-P. Vincent, and M. Lazdunski. 1982. Apamin as a selective blocker of the calcium-dependent potassium channel in neuroblastoma cells: voltage-clamp and biochemical characterization of the toxin receptor. *Proceedings of the National Academy of Sciences, USA.* 79:1308–1312.

Ishikawa, T., and D. I. Cook. 1993. A Ca^{2+}-activated Cl^- current in sheep parotid secretory cells. *Journal of Membrane Biology.* 135:261–171.

Joseph, S. K., A. P. Thomas, R. J. Williams, R. F. Irvine, and J. R. Williamson. 1984. *Myo*-inositol 1,4,5-triphosphate: a second messenger for the hormonal mobilization of intracellular Ca^{2+} in liver. *Journal of Biological Chemistry.* 259:3077–3081.

Joseph, S. K., and J. R. Williamson. 1986. Characteristics of inositol triphosphate-mediated Ca^{2+} release from permeabilized hepatocytes. *Journal of Biological Chemistry.* 261:14658–14664.

Koumi, S-i., R. Sato, T. Horikawa, T. Aramaki, H. Okumura. 1994. Characterization of the calcium-sensitive voltage-gated delayed rectifier potassium channel in isolated guinea pig hepatocytes. *Journal of General Physiology.* 104:1–27.

Koumi, S-i., R. Sato, T. Nagano, T. Horikawa, T. Aramaki, H. Okumura. 1991. Effective participation of Na^+/H^+ exchange on bile acid independent bile formation in guinea pig hepatocytes. *Biophysical Journal.* 59:93*a*. (Abstr.)

Kristensen, L. O. 1986. Associations between transports of alanine and cations across cell membrane in rat hepatocytes. *American Journal of Physiology.* 251:G575–G584.

Lynch, C. J., P. F. Blackmore, R. Charest, and J. H. Exton. 1985. The relationships between receptor binding capacity for norepinephrine, angiotensin II, and vasopressin and release of inositol triphosphate, Ca^{2+} mobilization, and phosphorylase activation in rat liver. *Molecular Pharmacology.* 28:93–99.

Marty, A., Y. P. Tan, and A. Trautmann. 1984. Three types of calcium-dependent channel in rat lacrimal glands. *Journal of Physiology.* 357:293–325.

Mauger, J. P., F. Poggioli, F. Guesdon, and M. Claret. 1984. Noradrenaline, vasopressin and angiotensin increase Ca^{2+} influx by opening a common pool of Ca^{2+} channels in isolated rat liver cells. *Biochemical Journal.* 221:121–127.

Mayer, M. L. 1985. A calcium-activated chloride current generates the after-depolarization of rat sensory neurons in culture. *Journal of Physiology.* 364:217–239.

Meier, P. J., A. Meier-Abt, C. Barrett, and J. L. Boyer. 1984. Mechanisms of taurocholate transport in canalicular and basolateral rat liver plasma membrane vesicles. Evidence for an electrogenic canalicular organic anion carrier. *Journal of Biological Chemistry.* 259:10614–10622.

Miledi, R. 1982. A calcium-dependent transient outward current in *Xenopus laevis* oocytes. *Proceedings of the Royal Society of London B Biological Sciences.* 215:491–497.

Miledi, R., and I. Parker. 1984. Chloride current induced by injection of calcium into *Xenopus* oocytes. *Journal of Physiology.* 357:173–183.

Ogden, D. C., T. Capiod, J. W. Walker, and D. R. Trentham. 1990. Kinetics of the conductance evoked by noradrenaline, inositol triphosphate or Ca^{2+} in guinea-pig isolated hepatocytes. *Journal of Physiology.* 422:585–602.

Orrenius, S., P. Nicotera, and G. Bellomo. 1987. Regulation of intracellular Ca^{2+} homeostasis in hepatocytes and toxicological consequences of its perturbation. *In* Modulation of Liver Cell Expression. W. Reutter, H. Popper, I. M. Arias, P. C. Heinrich, D. Keppler, and L. Landmann, editors. MTP Press Limited, Lancaster, UK. 157–164.

Owen, D. G., M. Segal, and J. L. Barker. 1984. A Ca-dependent Cl^- conductance in cultured mouse spinal neurons. *Nature.* 311:567–570.

Owen, D. G., M. Segal, and J. L. Barker. 1986. Voltage-clamp analysis of a Ca^{2+}- and voltage-dependent chloride conductance in cultured mouse spinal neurons. *Journal of Neurophysiology.* 55:1115–1135.

Pacaud, P., G. Loirand, J. L. Lavie, C. Mironneau, and J. Mironneau. 1989. Calcium-activated chloride current in rat vascular smooth muscle cells in short-term primary culture. *Pflügers Archiv.* 413:629–636.

Randriamampita, C., M. Chanson, and A. Trautmann. 1988. Calcium and secretagogues-induced conductances in rat exocrine pancreas. *Pflügers Archiv.* 411:53–57.

Sakmann, B., and E. Neher. 1983. Geometric parameters of pipettes and membrane patches. *In* Single-Channel Recording. B. Sakmann and E. Neher, editor. Plenum Publishing Corp., New York, NY. 37–51.

Soejima, M., and S. Kokubun. 1988. Single anion-selective channel and its ion selectivity in the vascular smooth muscle cell. *Pflügers Archiv.* 411:304–311.

Taylor, C. W., and J. W. Putney, Jr. 1985. Size of inositol 1,4,5-triphosphate-sensitive calcium pool in guinea-pig hepatocytes. *Biochemical Journal.* 232:435–438.

Wondergem, R., and D. R. Harder. 1980. Transmembrane potential and amino acid transport in rat hepatocytes in primary monolayer culture. *Journal of Cellular Physiology.* 104:53–60.

Zygmunt, A. C., and W. R. Gibbons. 1991. Calcium-activated chloride current in rabbit ventricular myocytes. *Circulation Research.* 68:424–437.

Zygmunt, A. C., and W. R. Gibbons. 1992. Properties of the calcium-activated chloride current in heart. *Journal of General Physiology.* 99:391–414.